Electronic Supplementary Information for

Revealing quantum mechanical effects in enzyme catalysis with large-scale electronic structure simulation

Zhongyue Yang[1], Rimsha Mehmood[1,2], Mengyi Wang[1,3], Helena W. Qi[1,2], Adam H. Steeves[1], and Heather J. Kulik[1,*]

[1]*Department of Chemical Engineering, Massachusetts Institute of Technology, Cambridge, MA 02139*

[2]*Department of Chemistry, Massachusetts Institute of Technology, Cambridge, MA 02139*

[3]*Department of Materials Science and Engineering, Massachusetts Institute of Technology, Cambridge, MA 02139*

Contents

Table S1. Missing Residues in DNMT1 added using Modeller.

Residue		Residue	
Name	**#**	**Name**	**#**
SER	645	LYS	1115
ASN	646	GLY	1116
GLU	852	LYS	1117
SER	853	GLY	1118
LEU	854	LYS	1119
LEU	855	PRO	1120
GLU	856	LYS	1121
GLY	857	SER	1122
ASP	858	GLN	1123
ASP	859	ALA	1124
VAL	956	CYS	1125
LYS	957	GLU	1126
ARG	958	PRO	1127
PRO	959	SER	1128
ARG	960	GLU	1129
ASP	978	PRO	1130
TYR	979	GLU	1131
ILE	980	ILE	1132
LYS	981	GLU	1133
GLY	982	ILE	1134
SER	983	GLU	1480
ASN	1108	ALA	1481
LYS	1109	GLY	1482
GLY	1110	LYS	1483
LYS	1111		
GLY	1112		
LYS	1113		
GLY	1114		

Table S2. Residue protonation states in DNMT1. If the residue is neutral, no value is indicated. The residues coordinated to Zn^{2+} ions were manually assigned charges and are shown in bold.

SER5		ALA97		HIE189		VAL281		ASP373	-1	SER465		LEU557		ARG649	+1	ALA741		ARG833	+1	LEU925	
ASN6		VAL98		SER190		LEU282		ILE374		PRO466		VAL558		MET650		SER742		GLY834		PHE926	
ALA7		LYS99	+1	LYS191	+1	TYR283		LYN375		GLY467		MET559		GLY651		ALA743		VAL835		GLY927	
PHE8		THR100		VAL192		TYR284		ILE376		ASN468		ALA560		TYR652		LEU744		**CY3836**		ASN928	
LYS9	+1	ASP101	-1	LYS193	+1	SER285		ARG377	+1	LYS469	+1	GLY561		GLN653		GLU745	-1	SER837		ILE929	
ARG10	+1	GLY102		VAL194		ALA286		VAL378		GLY470		GLU562	-1	CYS654		ILE746		**CY3838**		LEU930	
ARG11	+1	LYS103	+1	ILE195		THR287		ASN379		LYS471	+1	THR563		THR655		SER747		VAL839		ASP931	-1
ARG12	+1	LYS104	+1	TYR196		LYS288	+1	LYS380	+1	GLY472		THR564		PHE656		TYR748		GLU840	-1	LYS932	+1
CY113		SER105		LYS197	+1	ASN289		PHE381		LYS473	+1	ASN565		GLY657		ASN749		ALA841		HID933	
GLY14		TYR106		ALA198		GLY290		TYR382		GLY474		SER566		VAL658		GLY750		GLY842		ARG934	
VAL15		TYR107		PRO199		ILE291		ARG383	+1	LYS475	+1	ARG567	+1	LEU659		GLU751	-1	LYS843	+1	GLN935	
CY116		LYS108	+1	SER200		LEU292		PRO384		GLY476		GLY568		GLN660		PRO752		ALA844		VAL936	
GLU17		LYS109	+1	GLU201	-1	TYR293		GLU385	-1	LYS477	+1	GLN569		ALA661		GLN753		**CY3845**		GLY937	
VAL18		VAL110		ASN202		ARG294	+1	ASN386		GLY478		ARG570	+1	GLY662		SER754		ASP846	-1	ASN938	
CY119		CYS111		TRP203		VAL295		THR387		LYS479	+1	LEU571		GLN663		TRP755		PRO847		ALA939	
GLN20		ILE112		ALA204		GLY296		HIE388		PRO480		PRO572		TYR664		PHE756		ALA848		VAL940	
GLN21		ASP113	-1	MET205		ASP297	-1	LYS389	+1	LYS481	+1	GLN573		GLY665		GLN757		ALA849		PRO941	
PRO22		ALA114		GLU206	-1	GLY298		SER390		SER482		LYN574		VAL666		ARG758	+1	ARG850	+1	PRO942	
GLU23	-1	GLU115	-1	GLY207		VAL299		THR391		GLN483		GLY575		ALA667		GLN759		GLN851		PRO943	
CY124		THR116		GLY208		TYR300		PRO392		ALA484		ASP576	-1	GLN668		LEU760		PHE852		LEU944	
GLY25		LEU117		MET209		LEU301		ALA393		CYS485		VAL577		THR669		ARG761	+1	ASN853		ALA945	
LYS26	+1	GLU118	-1	ASP210	-1	PRO302		SER394		GLU486	-1	GLU578	-1	ARG670	+1	GLY762		THR854		LYS946	+1
CY127		VAL119		PRO211		PRO303		TYR395		PRO487		MET579		ARG671	+1	ALA763		LEU855		ALA947	
LYS28	+1	GLY120		GLU212	-1	GLU304	-1	HIE396		SER488		LEU580		ARG672	+1	GLN764		ILE856		ILE948	
ALA29		ASP121	-1	SER213		ALA305		ALA397		GLU489	-1	CYS581		ALA673		TYR765		PRO857		GLY949	
CY130		CYS122		LEU214		PHE306		ASP398	-1	PRO490		GLY582		ILE674		GLN766		TRP858		LEU950	
LYS31	+1	VAL123		LEU215		THR307		ILE399		GLU491	-1	GLY583		ILE675		PRO767		CYS859		GLU951	-1
ASP32	-1	SER124		GLH216		PHE308		ASN400		ILE492		PRO584		LEU676		ILE768		LEU860		ILE952	
MET33		VAL125		GLY217		ASN309		LEU401		GLU493	-1	PRO585		ALA677		LEU769		PRO861		LYS953	+1
VAL34		ILE126		ASP218	-1	ILE310		LEU402		ILE494		CYS586		ALA678		ARG770	+1	**HD1862**		LEU954	
LYS35	+1	PRO127		ASP219	-1	LYS311	+1	TYR403		LYS495	+1	GLN587		ALA679		ASP771	-1	THR863		CYS955	
PHE36		ASP128	-1	GLY220		LEU312		TRP404		LEU496		GLY588		PRO680		HIE772		GLY864		MET956	
GLY37		ASP129	-1	LYS221	+1	SER313		SER405		PRO497		PHE589		GLY681		ILE773		ASN865		LEU957	
GLY38		SER130		THR222		SER314		ASP406	-1	LYS498	+1	SER590		GLU682	-1	CYS774		ARG866	+1	ALA958	
SER39		SER131		TYR223		PRO315		GLU407	-1	LEU499		GLY591		LYS683	+1	LYS775	+1	HIE867		LYS959	+1
GLY40		LYS132	+1	PHE224		VAL316		GLU408	-1	ARG500	+1	MET592		LEU684		ASP776	-1	ASN868		ALA960	
ARG41	+1	PRO133		TYR225		LYS317	+1	ALA409		THR501		ASN593		PRO685		MET777		HIE869			
SER42		LEU134		GLN226		ARG318	+1	VAL410		LEU502		ARG594	+1	LEU686		SER778		TRP870			
LYS43	+1	TYR135		LEU227		PRO319		VAL411		ASH503		PHE595		PHE687		ALA779		ALA871			
GLN44		LEU136		TRP228		ARG320	+1	ASP412	-1	VAL504		ASN596		PRO688		LEU780		GLY872			
ALA45		ALA137		TYR229		LYS321	+1	PHE413		PHE505		SER597		GLU689	-1	VAL781		LEU873			
CY146		ARG138	+1	ASP230	-1	GLU322	-1	LYS414	+1	SER506		ARG598	+1	PRO690		ALA782		TYR874			
GLN47		VAL139		GLN231		PRO323		ALA415		GLY507		THR599		LEU691		ALA783		GLY875			
GLU48	-1	THR140		ASP232	-1	VAL324		VAL416		CYS508		TYR600		HID692		ARG784	+1	ARG876	+1		
ARG49	+1	ALA141		TYR233		ASP325	-1	GLN417		GLY509		SER601		VAL693		MET785		LEU877			
ARG50	+1	LEU142		ALA234		GLU326	-1	GLY418		GLY510		LYN602		PHE694		ARG786	+1	GLU878	-1		
CY151		TRP143		ARG235	+1	ASP327	-1	ARG419	+1	LEU511		PHE603		ALA695		HIE787		TRP879			
PRO52		GLU144	-1	PHE236		LEU328		CYS420		SER512		LYN604		PRO696		ILE788		ASP880	-1		
ASN53		ASP145	-1	GLU237	-1	TYR329		THR421		GLU513	-1	ASN605		ARG697	+1	PRO789		GLY881			
MET54		SER146		SER238		PRO330		VAL422		GLY514		SER606		ALA698		LEU790		PHE882			
ALA55		SER147		PRO239		GLU331	-1	GLU423	-1	PHE515		LEU607		CYS699		ALA791		PHE883			
MET56		ASN148		PRO240		HIE332		TYR424		HID516		VAL608		GLN700		PRO792		SER884			
LYS57	+1	GLY149		LYS241	+1	TYR333		GLY425		GLN517		VAL609		LEU701		GLY793		THR885			
GLU58	-1	GLN150		THR242		ARG334	+1	GLU426	-1	ALA518		SER610		SER702		SER794		THR886			
ALA59		MET151		GLN243		LYS335	+1	ASP427	-1	GLY519		PHE611		VAL703		ASP795	-1	VAL887			
ASH60		PHE152		PRO244		TYR336		LEU428		ILE520		LEU612		VAL704		TRP796		THR888			
ASP61	-1	**HD1153**		THR245		SER337		PRO429		SER521		SER613		VAL705		ARG797	+1	ASN889			
ASP62	-1	ALA154		GLU246	-1	ASP338	-1	GLU430	-1	ASP522	-1	TYR614		ASP706	-1	ASH798		PRO890			
GLU63	-1	HIE155		ASP247	-1	TYR339		CYS431		THR523		CYS615		ASP707	-1	LEU799		GLU891	-1		
GLU64	-1	TRP156		ASN248		ILE340		VAL432		LEU524		ASH616		LYS708	+1	PRO800		PRO892			
VAL65		PHE157		LYS249	+1	LYS341	+1	GLN433		TRP525		TYR617		LYS709	+1	ASN801		MET893			
ASH66		CYS158		PHE250		GLY342		VAL434		ALA526		TYR618		PHE710		ILE802		GLY894			
ASP67	-1	ALA159		LYS251	+1	SER343		TYR435		ILE527		ARG619	+1	VAL711		GLU803	-1	LYN895			
ASN68		GLY160		PHE252		ASN344		SER436		GLU528	-1	PRO620		SER712		VAL804		GLN896			

Table S2 (continued). Residue protonation states in DNMT1. If the residue is neutral, no value is indicated. The residues coordinated to Zn^{2+} ions were manually assigned charges and are shown in bold.

ILE69		THR161		**CY3253**		LEU345		MET437		MET529		ARG621	+1	ASN713		ARG805	+1	GLY897			
PRO70		ASP162	-1	VAL254		ASP346	-1	GLY438		TRP530		PHE622		ILE714		LEU806		ARG898	+1		
GLU71	-1	THR163		SER255		ALA347		GLY439		ASP531	-1	PHE623		THR715		SER807		VAL899			
MET72		VAL164		**CY3256**		PRO348		PRO440		PRO532		LEU624		ARG716	+1	ASP808	-1	LEU900			
PRO73		LEU165		ALA257		GLU349	-1	ASN441		ALA533		LEU625		LEU717		GLY809		HIE901			
SER74		GLY166		ARG258	+1	PRO350		ARG442	+1	ALA534		GLU626	-1	SER718		THR810		PRO902			
PRO75		ALA167		LEU259		TYR351		PHE443		GLN535		ASN627		SER719		MET811		GLU903	-1		
LYS76	+1	THR168		ALA260		ARG352	+1	TYR444		ALA536		VAL628		GLY720		ALA812		GLN904			
LYN77		SER169		GLU261	-1	ILE353		PHE445		PHE537		ARG629	+1	PRO721		ARG813	+1	HIE905			
MET78		ASP170	-1	MET262		GLY354		LEU446		ARG538	+1	ASN630		PHE722		LYN814		ARG906	+1		
HIE79		PRO171		ARG263	+1	ARG355	+1	GLU447	-1	LEU539		PHE631		ARG723	+1	LEU815		VAL907			
GLN80		LEU172		GLN264		ILE356		ALA448		ASN540		VAL632		THR724		ARG816	+1	VAL908			
GLY81		GLU173	-1	LYS265	+1	LYS357	+1	TYR449		ASN541		SER633		ILE725		TYR817		SER909			
LYS82	+1	LEU174		GLU266	-1	GLU358	-1	ASN450		PRO542		PHE634		THR726		THR818		VAL910			
LYS83	+1	PHE175		ILE267		ILE359		ALA451		GLY543		LYN635		VAL727		HIE819		ARG911	+1		
LYN84		LEU176		PRO268		PHE360		LYS452	+1	SER544		ARG636	+1	ARG728	+1	HIE820		GLU912	-1		
LYS85	+1	VAL177		ARG269	+1	CYS361		SER453		THR545		SER637		ASP729	-1	ASP821	-1	CYS913			
GLN86		ASP178	-1	VAL270		PRO362		LYS454	+1	VAL546		MET638		THR730		ARG822	+1	ALA914			
ASN87		GLH179		LEU271		LYN363		SER455		PHE547		VAL639		MET731		LYS823	+1	ARG915	+1		
LYS88	+1	**CY3180**		GLU272	-1	LYS364	+1	PHE456		THR548		LEU640		SER732		ASN824		SER916			
ASN89		GLU181	-1	GLN273		SER365		GLU457	-1	GLH549		LYS641	+1	ASP733	-1	GLY825		GLN917			
ARG90	+1	ASP182	-1	LEU274		ASN366		ASP458	-1	ASP550	-1	LEU642		LEU734		ARG826	+1	GLY918			
ILE91		MET183		GLU275	-1	GLY367		PRO459		CYS551		THR643		PRO735		SER827		PHE919			
SER92		GLN184		ASP276	-1	ARG368	+1	PRO460		ASN552		LEU644		GLU736	-1	SER828		PRO920			
TRP93		LEU185		LEU277		PRO369		ASN461		ILE553		ARG645	+1	VAL737		SER829		ASP921	-1		
VAL94		SER186		ASP278	-1	ASN370		HID462		LEU554		CYS646		ARG738	+1	GLY830		THR922			
GLY95		TYR187		SER279		GLH371		ALA463		LEU555		LEU647		ASN739		ALA831		TYR923			
GLU96	-1	ILE188		ARG280	+1	THR372		ARG464	+1	LYS556	+1	VAL648		GLY740		LEU832		ARG924	+1		

Table S3. Residue protonation states in CutC. The residue ASP216 is manually assigned as ASH216 from the experimental hypothesis that TMA could be protonated by that aspartic acid.

Res	q	Res	q	Res	q	Res	q	Res	q	Res	q	Res	q
GLY53	0	VAL167	0	GLU281	-1	PHE395	0	TRP509	0	LYS623	1	GLY737	0
ILE54	0	LEU168	0	LEU282	0	VAL396	0	PRO510	0	LYS624	1	PRO738	0
PRO55	0	ARG169	1	ALA283	0	ASN397	0	ILE511	0	LEU625	0	THR739	0
ASP56	-1	GLU170	-1	ALA284	0	MET398	0	CYS512	0	VAL626	0	ALA740	0
GLY57	0	GLU171	-1	ARG285	1	CYS399	0	ILE513	0	TYR627	0	ILE741	0
PRO58	0	VAL172	0	GLU286	-1	VAL400	0	GLU514	-1	ASP628	-1	ILE742	0
THR59	0	PHE173	0	THR287	0	GLY401	0	LEU515	0	ASP629	-1	LYS743	1
PRO60	0	PRO174	0	ASP288	-1	GLY402	0	VAL516	0	ARG630	1	SER744	0
ARG61	1	PHE175	0	PRO289	0	VAL403	0	LEU517	0	LYS631	1	VAL745	0
HIE62	0	TRP176	0	ARG290	1	THR404	0	ASN518	0	TYR632	0	SER746	0
VAL63	0	GLN177	0	ARG291	1	ARG405	1	HID519	0	THR633	0	LYS747	1
LYS64	1	ASN178	0	LYS292	1	GLU406	-1	GLY520	0	LEU634	0	MET748	0
LEU65	0	LYS179	1	ALA293	0	GLY407	0	VAL521	0	ALA635	0	ALA749	0
LYS66	1	SER180	0	GLU294	-1	HID408	0	PRO522	0	GLN636	0	ASN750	0
GLU67	-1	VAL181	0	LEU295	0	ASP409	-1	LEU523	0	LEU637	0	ASP751	-1
ASN68	0	ASP182	-1	GLN296	0	ALA410	0	TRP524	0	ASN638	0	ASN752	0
PHE69	0	GLU183	-1	LYS297	1	THR411	0	TYR525	0	GLU639	-1	MET753	0
LEU70	0	PHE184	0	ILE298	0	ASN412	0	GLY526	0	ALA640	0	ASN754	0
LYS71	1	CYS185	0	SER299	0	ASP413	-1	ALA527	0	LEU641	0	ILE755	0
GLN72	0	GLU186	-1	GLU300	-1	LEU414	0	LYS528	1	LYS642	1	GLY756	0
VAL73	0	GLY187	0	VAL301	0	THR415	0	VAL529	0	ALA643	0	MET757	0

Res	q	Res	q	Res	q	Res	q	Res	q	Res	q	Res	q
PRO74	0	GLN188	0	ASN302	0	TYR416	0	THR530	0	ASP644	-1	VAL758	0
SER75	0	TYR189	0	ALA303	0	MET417	0	PRO531	0	PHE645	0	HIE759	0
ILE76	0	ARG190	1	ARG304	1	LEU418	0	ASP532	-1	ALA646	0	ASN760	0
THR77	0	GLU191	-1	VAL305	0	MET419	0	MET533	0	GLY647	0	PHE761	0
VAL78	0	ALA192	0	PRO306	0	ASP420	-1	GLY534	0	TYR648	0	LYS762	1
GLN79	0	ASP193	-1	ALA307	0	ALA421	0	ASP535	-1	ASP649	-1	LEU763	0
ARG80	1	LEU194	0	HIE308	0	VAL422	0	LEU536	0	GLN650	0	MET764	0
ALA81	0	TRP195	0	ALA309	0	ARG423	1	SER537	0	ILE651	0	SER765	0
VAL82	0	GLU196	-1	PRO310	0	HID424	0	GLN538	0	LEU652	0	GLY766	0
ALA83	0	MET197	0	SER311	0	VAL425	0	TYR539	0	ALA653	0	LEU767	0
ILE84	0	SER198	0	ASN312	0	ARG426	1	ASP540	-1	ASP654	-1	LEU768	0
THR85	0	GLY199	0	PHE313	0	ILE427	0	THR541	0	CYS655	0	ASP769	-1
LYS86	1	GLU200	-1	TRP314	0	TYR428	0	TYR542	0	LEU656	0	THR770	0
ILE87	0	SER201	0	GLU315	-1	GLN429	0	GLU543	-1	ALA657	0	PRO771	0
ALA88	0	PHE202	0	ALA316	0	PRO430	0	LYS544	1	ALA658	0	GLU772	-1
LYS89	1	VAL203	0	ILE317	0	THR431	0	PHE545	0	PRO659	0	GLY773	0
GLU90	-1	SER204	0	GLN318	0	LEU432	0	GLU546	-1	LYS660	1	GLU774	-1
ASN91	0	ASP205	-1	ALA319	0	ALA433	0	ALA547	0	TYR661	0	ASN775	0
PRO92	0	CYS206	0	VAL320	0	THR434	0	ALA548	0	GLY662	0	GLY776	0
GLY93	0	SER207	0	TRP321	0	ARG435	1	VAL549	0	ASN663	0	LEU777	0
LEU94	0	TYR208	0	THR322	0	VAL436	0	LYS550	1	ASP664	-1	ILE778	0
PRO95	0	HIP209	0	VAL323	0	HIE437	0	GLU551	-1	ASP665	-1	THR779	0
LYS96	1	ALA210	0	GLU324	-1	ASN438	0	GLN552	0	ASP666	-1	LEU780	0
PRO97	0	VAL211	0	SER325	0	LYS439	1	ILE553	0	TYR667	0	ILE781	0
LEU98	0	ASN212	0	LEU326	0	SER440	0	ARG554	1	ALA668	0	ARG782	1
LEU99	0	GLY213	0	LEU327	0	PRO441	0	TRP555	0	ASP669	-1	THR783	0
ARG100	1	GLY214	0	VAL328	0	GLN442	0	ILE556	0	MET670	0	ALA784	0
ALA101	0	GLY215	0	VAL329	0	LYS443	1	THR557	0	ILE671	0	CYS785	0
LYS102	1	**ASH216**	**0**	GLU330	-1	TYR444	0	LYS558	1	ALA672	0	MET786	0
THR103	0	SER217	0	GLU331	-1	LEU445	0	ASN559	0	ALA673	0	LEU787	0
PHE104	0	ASN218	0	ASN332	0	LYS446	1	THR560	0	ASP674	-1	GLY788	0
ARG105	1	PRO219	0	GLN333	0	LYS447	1	SER561	0	LEU675	0	ASN789	0
TYR106	0	GLY220	0	THR334	0	ILE448	0	VAL562	0	VAL676	0	GLY790	0
CYS107	0	TYR221	0	GLY335	0	VAL449	0	ALA563	0	HIE677	0	GLU791	-1
CYS108	0	ASP222	-1	MET336	0	ASP450	-1	THR564	0	PHE678	0	MET792	0
GLU109	-1	VAL223	0	SER337	0	VAL451	0	VAL565	0	THR679	0	GLN793	0
THR110	0	ILE224	0	ILE338	0	ILE452	0	ILE566	0	GLU680	-1	PHE794	0
ALA111	0	LEU225	0	GLY339	0	ARG453	1	SER567	0	THR681	0	ASN795	0
PRO112	0	MET226	0	ARG340	1	SER454	0	GLN568	0	GLU682	-1	TYR796	0
LEU113	0	LYS227	1	VAL341	0	GLY455	0	ARG569	1	HID683	0	LEU797	0
VAL114	0	LYS228	1	ASP342	-1	MET456	0	ALA570	0	ARG684	1	ASP798	-1
ILE115	0	GLY229	0	GLN343	0	GLY457	0	HIE571	0	LYS685	1	ASN799	0
GLN116	0	MET230	0	TYR344	0	PHE458	0	ARG572	1	TYR686	0	GLU800	-1
ASP117	-1	LEU231	0	MET345	0	PRO459	0	GLU573	-1	LYS687	1	LEU801	0
HIE118	0	ASP232	-1	TYR346	0	ALA460	0	LEU574	0	THR688	0	LEU802	0
GLU119	-1	ILE233	0	PRO347	0	VAL461	0	ALA575	0	LEU689	0	LEU803	0
LEU120	0	GLN234	0	PHE348	0	HID462	0	PRO576	0	TYR690	0	ASP804	-1

Res	q	Res	q	Res	q	Res	q	Res	q	Res	q	Res	q
ILE121	0	ARG235	1	TYR349	0	PHE463	0	LYS577	1	SER691	0	ALA805	0
VAL122	0	GLU236	-1	ARG350	1	ASP464	-1	PRO578	0	VAL692	0	GLN806	0
GLY123	0	ALA237	0	ALA351	0	ASP465	-1	LEU579	0	LEU693	0	LYS807	1
SER124	0	ARG238	1	ASP352	-1	ALA466	0	MET580	0	SER694	0	HIE808	0
PRO125	0	GLU239	-1	ILE353	0	HID467	0	SER581	0	HID695	0	PRO809	0
ASN126	0	LYS240	1	ASP354	-1	ILE468	0	LEU582	0	GLY696	0	GLU810	-1
GLY127	0	LEU241	0	SER355	0	LYS469	1	MET583	0	THR697	0	LYS811	1
ALA128	0	GLU242	-1	GLY356	0	MET470	0	TYR584	0	LEU698	0	TYR812	0
PRO129	0	GLN243	0	ARG357	1	MET471	0	GLU585	-1	SER699	0	ARG813	1
ARG130	1	LEU244	0	LEU358	0	LEU472	0	GLY586	0	ILE700	0	ASP814	-1
ALA131	0	ASP245	-1	THR359	0	ALA473	0	CYS587	0	SER701	0	LEU815	0
GLY132	0	TYR246	0	GLU360	-1	LYS474	1	MET588	0	ASN702	0	VAL816	0
ALA133	0	ALA247	0	TYR361	0	GLY475	0	GLU589	-1	ASN703	0	VAL817	0
PHE134	0	ASN248	0	GLU362	-1	VAL476	0	SER590	0	THR704	0	ARG818	1
SER135	0	PRO249	0	ALA363	0	SER477	0	GLY591	0	PRO705	0	VAL819	0
PRO136	0	GLU250	-1	PHE364	0	ILE478	0	ARG592	1	PHE706	0	ALA820	0
GLU137	-1	ASP251	-1	ASP365	-1	GLU479	-1	ASP593	-1	GLY707	0	GLY821	0
VAL138	0	ILE252	0	LEU366	0	ASP480	-1	VAL594	0	GLN708	0	TYR822	0
ALA139	0	ASP253	-1	ALA367	0	ALA481	0	SER595	0	LEU709	0	SER823	0
TRP140	0	LYS254	1	GLY368	0	ARG482	1	ALA596	0	LEU710	0	ALA824	0
ARG141	1	ILE255	0	CYS369	0	ASP483	-1	GLY597	0	GLY711	0	PHE825	0
TRP142	0	TYR256	0	MET370	0	TYR484	0	GLY598	0	ALA712	0	PHE826	0
LEU143	0	PHE257	0	LEU371	0	CYS485	0	ALA599	0	SER713	0	VAL827	0
GLN144	0	TYR258	0	VAL372	0	LEU486	0	MET600	0	ALA714	0	GLU828	-1
ASP145	-1	LYS259	1	LYS373	1	MET487	0	TYR601	0	ASN715	0	LEU829	0
GLU146	-1	SER260	0	MET374	0	GLY488	0	ASN602	0	GLY716	0	CYS830	0
LEU147	0	VAL261	0	SER375	0	CYS489	0	PHE603	0	ARG717	1	LYS831	1
ASP148	-1	ILE262	0	GLU376	-1	VAL490	0	GLY604	0	ARG718	1	ASP832	-1
THR149	0	GLU263	-1	MET377	0	GLU491	-1	PRO605	0	ALA719	0	VAL833	0
ILE150	0	THR264	0	MET378	0	PRO492	0	GLY606	0	TRP720	0	GLN834	0
GLY151	0	ALA265	0	TRP379	0	GLN493	0	VAL607	0	MET721	0	ASP835	-1
SER152	0	GLU266	-1	ILE380	0	LYS494	1	VAL608	0	PRO722	0	GLU836	-1
ARG153	1	GLY267	0	THR381	0	SER495	0	TRP609	0	LEU723	0	ILE837	0
PRO154	0	VAL268	0	SER382	0	GLY496	0	SER610	0	SER724	0	ILE838	0
GLN155	0	MET269	0	GLU383	-1	ARG497	1	GLY611	0	ASP725	-1	SER839	0
ASP156	-1	ILE270	0	GLY384	0	LEU498	0	LEU612	0	GLY726	0	ARG840	1
PRO157	0	TYR271	0	ALA385	0	TYR499	0	ALA613	0	ILE727	0	THR841	0
PHE158	0	ALA272	0	SER386	0	GLN500	0	THR614	0	SER728	0	MET842	0
TYR159	0	ARG273	1	LYS387	1	TRP501	0	TYR615	0	PRO729	0	LEU843	0
ILE160	0	ARG274	1	PHE388	0	THR502	0	VAL616	0	THR730	0	HIE844	0
SER161	0	LEU275	0	PHE389	0	SER503	0	ASP617	-1	GLN731	0	GLY845	0
GLU162	-1	SER276	0	ALA390	0	THR504	0	SER618	0	GLY732	0	PHE846	0
GLU163	-1	ALA277	0	GLY391	0	GLY505	0	MET619	0	ALA733	0	**CHT847**	**1**
ASP164	-1	TYR278	0	TYR392	0	TYR506	0	ALA620	0	ASP734	-1		
LYS165	1	ALA279	0	GLN393	0	THR507	0	ALA621	0	TYR735	0		
LYS166	1	ALA280	0	PRO394	0	GLN508	0	ILE622	0	LYS736	1		

Table S4. Overall charge assignment to DNMT structure.

Component	Charge
Positive amino acids	+126
Negative amino acids	-121
DNA	-21
Zn1 site	-1
Zn2 site	-2
Zn3 site	-1
Zn4 site	-2
Total	**-22**

Table S5. Overall charge assignment to CutC structure.

Component	Charge
Positive amino acids	+84
Negative amino acids	-104
Choline	+1
Total	**-19**

Table S6. Charges assigned to Zn^{2+} sites according to Zinc Amber Force Field.

Sites 1 (and 3)		
Residue	Residue number	Charge
Zn1 (Zn3)	1 (3)	0.84
HID	862 (153)	0.14
CYS	838 (180)	-0.66
CYS	845 (256)	-0.66
CYS	836 (253)	-0.66
	Total	**-1.00**
Sites 2 (and 4)		
Zn2 (Zn4)	2 (4)	0.52
CYS	13 (46)	-0.63
CYS	16 (30)	-0.63
CYS	19 (24)	-0.63
CYS	51 (27)	-0.63
	Total	**-2.0**

Table S7. QM residues included in CSA region and selected after with # atoms and charge.

Res. #	Res.	# At	Charge	CSA?		Large QM
				Before	After	
208	TYR	21	0	Y	Y	Y
209	HIP	18	1	Y	--	Y
212	ASN	14	0	Y	--	Y
213	GLY	7	0	Y	--	Y
214	GLY	7	0	Y	--	Y
215	GLY	7	0	Y	--	Y
216	ASH	13	0	Y	Y	Y
217	SER	11	0	Y	--	Y
218	ASN	14	0	Y	--	Y
219	*PRO*	*14*	*0*	--	--	Y
327	*LEU*	*19*	*0*	--	--	Y
332	*ASN*	*14*	*0*	--	--	Y
333	GLN	17	0	Y	Y	Y
334	THR	14	0	Y	--	Y
335	GLY	7	0	Y	--	Y
336	MET	17	0	Y	Y	Y
337	SER	11	0	Y	--	Y
379	TRP	24	0	Y	--	Y
381	THR	14	0	Y	--	Y
385	ALA	10	0	Y	--	Y
388	PHE	20	0	Y	--	Y
389	PHE	20	0	Y	Y	Y
390	*ALA*	*10*	*0*	--	--	Y
393	GLN	17	0	Y	Y	Y
394	PRO	14	0	Y	--	Y
395	PHE	20	0	Y	--	Y
396	VAL	16	0	Y	--	Y
397	ASN	14	0	Y	--	Y
429	GLN	17	0	Y	--	Y
431	THR	14	0	Y	--	Y
462	*HID*	*17*	*0*	--	--	Y
486	LEU	19	0	Y	--	Y
487	MET	17	0	Y	--	Y
488	GLY	7	0	Y	Y	Y
489	CYS	11	0	Y	Y	Y
490	VAL	16	0	Y	Y	Y
491	GLU	15	-1	Y	Y	Y
492	PRO	14	0	Y	--	Y
493	GLN	17	0	Y	--	Y
499	*TYR*	*21*	*0*	--	--	Y
500	GLN	17	0	Y	--	Y
501	TRP	24	0	Y	Y	Y
502	THR	14	0	Y	--	Y
503	SER	11	0	Y	--	Y
504	THR	14	0	Y	--	Y
505	GLY	7	0	Y	--	Y
506	TYR	21	0	Y	--	Y
580	MET	17	0	Y	--	Y

Res. #	Res.	# At	Charge	CSA?		Large QM
605	PRO	14	0	Y	--	Y
606	GLY	7	0	Y	--	Y
607	*VAL*	*16*	*0*	--	--	Y
608	VAL	16	0	Y	--	Y
696	GLY	7	0	Y	--	Y
697	THR	14	0	Y	--	Y
698	LEU	19	0	Y	--	Y
699	SER	11	0	Y	--	Y
700	ILE	19	0	Y	--	Y
701	SER	11	0	Y	--	Y
702	ASN	14	0	Y	--	Y
755	ILE	19	0	Y	--	Y
756	GLY	7	0	Y	--	Y
757	MET	17	0	Y	--	Y
758	VAL	16	0	Y	--	Y
818	*ARG*	*24*	*1*	--	--	Y
819	*VAL*	*16*	*0*	Y	Y	--
820	ALA	10	0	Y	Y	Y
821	GLY	7	0	Y	Y	Y
822	TYR	21	0	Y	Y	Y
823	*SER*	*11*	*0*	Y	Y	--
847	CHT	21	1	Y	Y	Y
872	WAT	3	0	Y	--	--
874	WAT	3	0	Y	--	--
875	WAT	3	0	Y	--	--
879	WAT	3	0	Y	--	--
882	WAT	3	0	Y	--	--
883	WAT	3	0	Y	--	--
886	WAT	3	0	Y	--	--
891	WAT	3	0	Y	--	--
894	WAT	3	0	Y	--	--
898	WAT	3	0	Y	--	--
902	WAT	3	0	Y	--	--
908	WAT	3	0	Y	--	--
965	WAT	3	0	Y	--	--
976	WAT	3	0	Y	--	--
977	WAT	3	0	Y	--	--
1052	WAT	3	0	Y	--	--
1524	WAT	3	0	Y	--	--
5044	WAT	3	0	Y	--	--
7696	WAT	3	0	Y	--	--
Totals			# atoms	926	263	1003
			with link	962	281	1043
			charge	1	0	2

Table S8. Comparison of isolated choline, hemiaminal intermediate, acetaldehyde and TMA (closed shell) species along with radicals (choline, choline O-centered radical, hemiaminal radical, hemiaminal O-centered radical, acetaldehyde radical) in the gas phase (GP), with a dielectric of 4 to represent the protein environment implicitly, and with thermodynamic T = 300 K corrections. All properties are evaluated at the ωPBEh/6-311++G** level of theory and reveal that although the hemiaminal intermediate is more stable than choline, its radical is much less stable.

Species	GP	ε=4	$+\Delta G_{gas}$
choline	3.5	4.8	**5.6**
Hemiaminal int (enant/orig)	0	0	**0**
acetaldehyde and trimethylammonium	14.7	7.6	**5.0**

Species	GP	ε=4	$+\Delta G_{gas}$
choline radical	0	0	**0**
choline O radical	18.0	15.5	**14.5**
Hemiaminal radical (enant/ orig)	8.3	7.7	**6.4**
Hemiaminal O radical	12.0	11.0	**10.7**
acetaldehyde radical and trimethylammonium	15.2	7.0	**6.0**

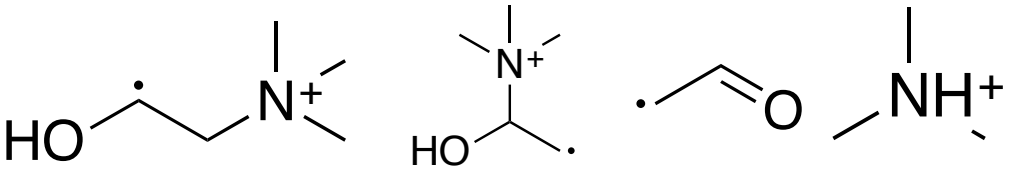

Choline radical **Hemiaminal radical** **Acetaldehyde radical and TMA**

Figure S1. Structures of the hemiaminal intermediate and radical as well as choline and dissociated products.

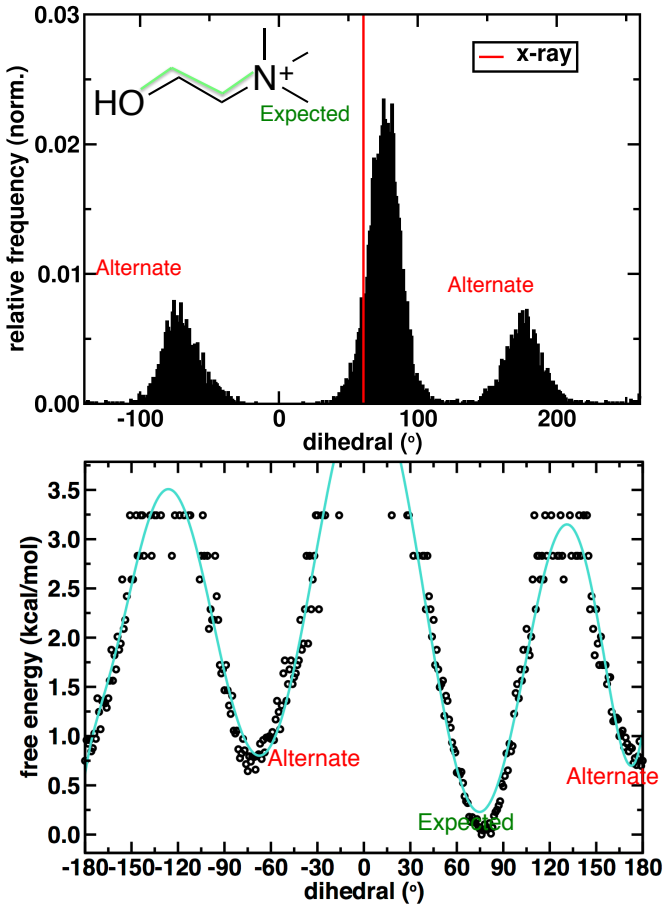

Figure S2. Choline dihedral sampled during 100 ns of NpT MD: top is relative frequency and bottom is estimated free energy via –kTln<P>. The dihedral is shown in inset.

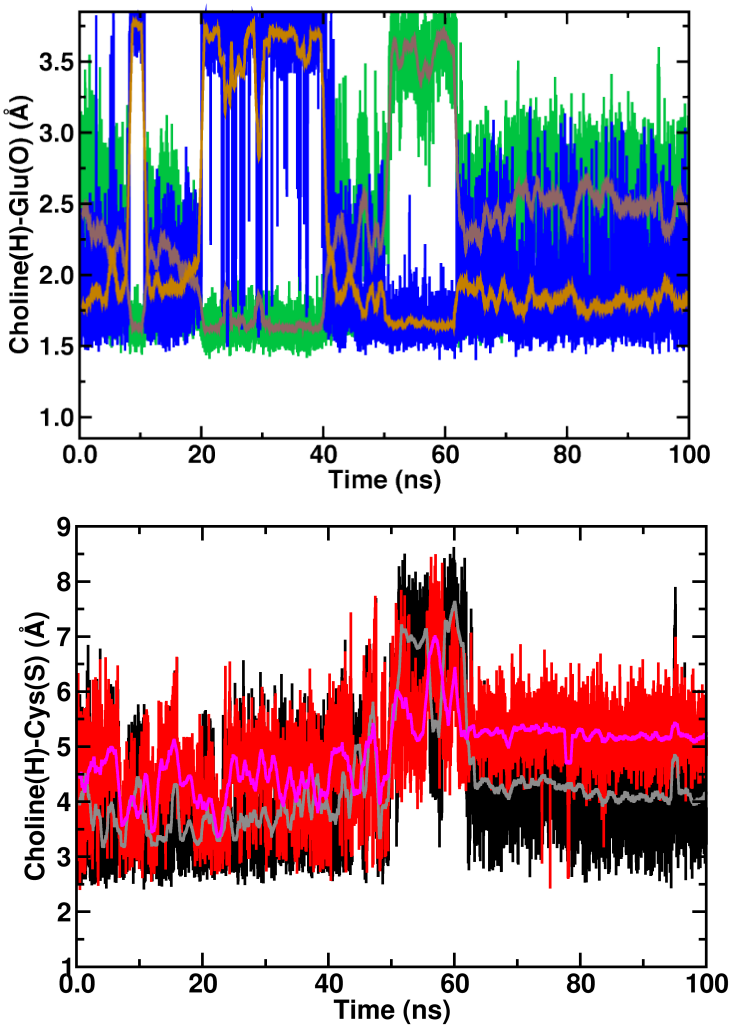

Figure S3. Distances sampled during 100 ns of NpT MD: top is Glu O^- to choline hydroxyl H distance with a running average also shown (green and blue represent the two different O^- atoms of Glu) and bottom is the distance of the choline H to be abstracted to the abstracting Cys S (Cys is not in radical form during dynamics, as the protein is in the resting state).

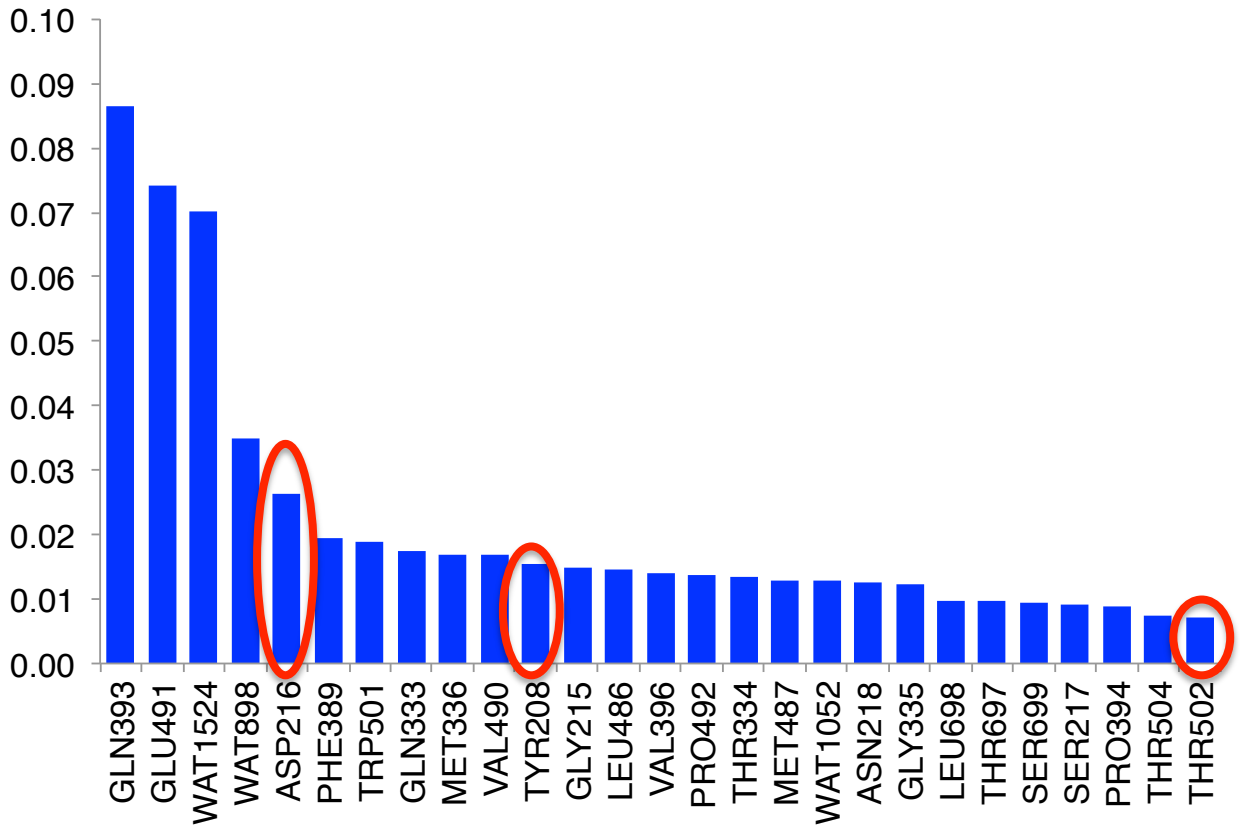

Figure S4. Ranked charge shifts from 962 atom QM region in CSA. Selected residues were identified as essential from experiment and marked with red circles.

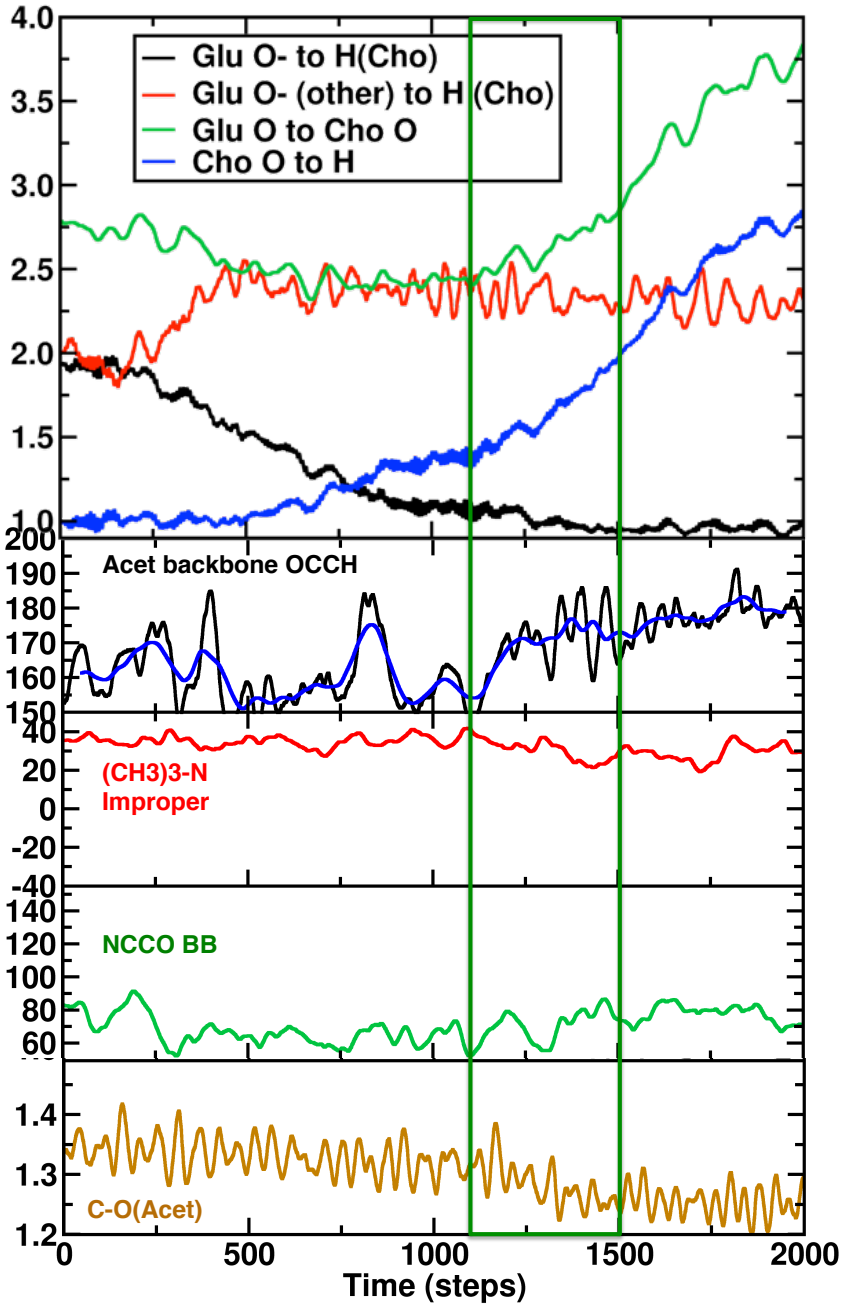

Figure S5. Additional geometric characteristics of the forced Cholinyl radical deprotonation.

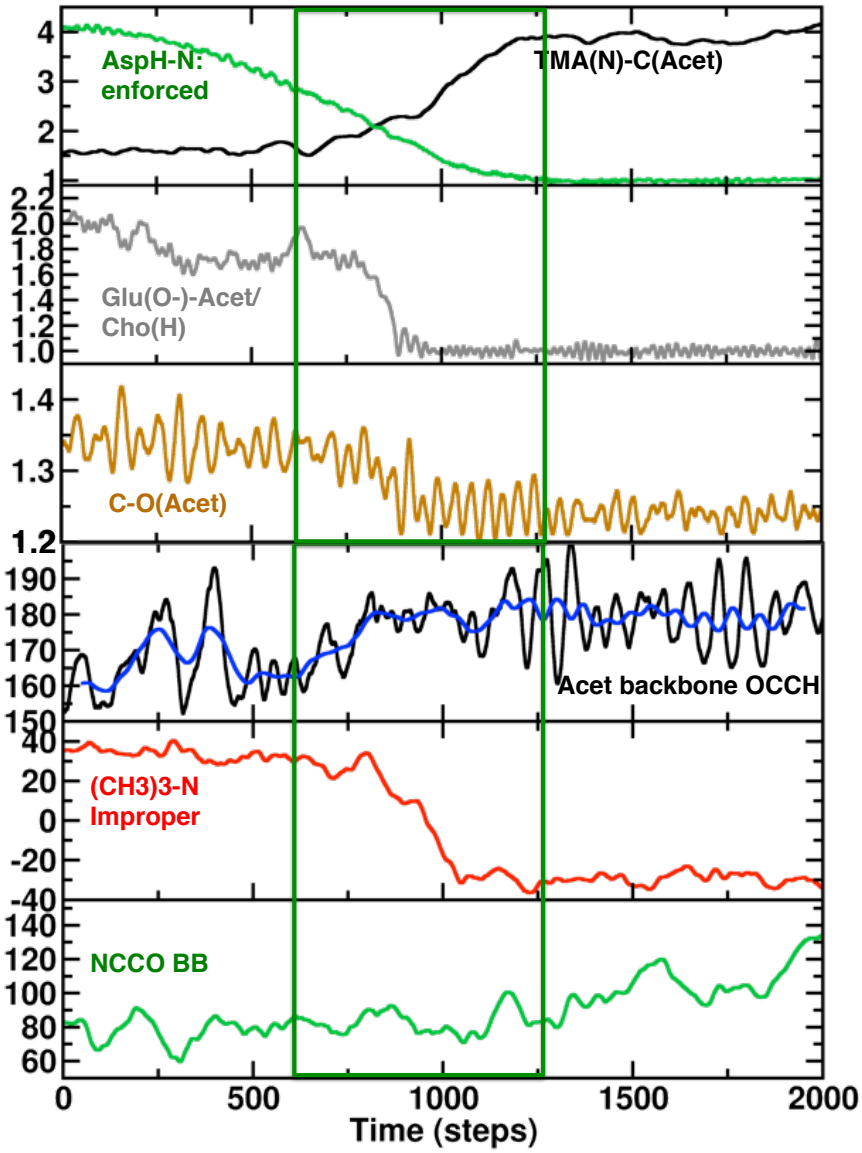

Figure S6. Forced TMA protonation geometric properties for SMD.

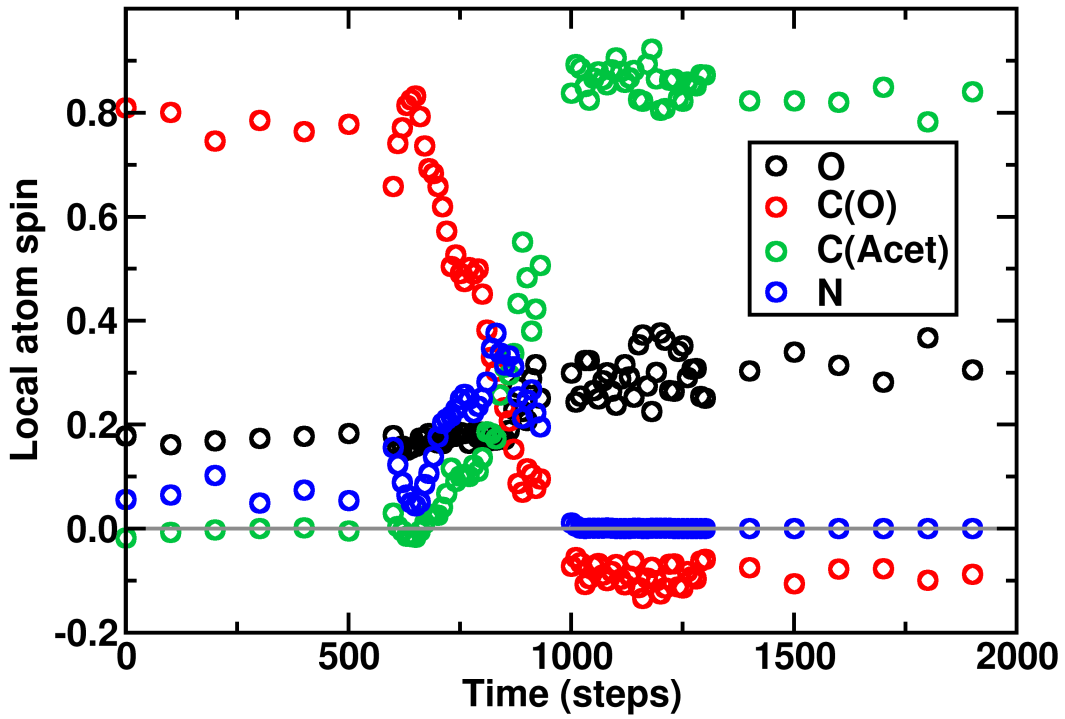

Figure S7. Spins during forced Choline radical protonation.

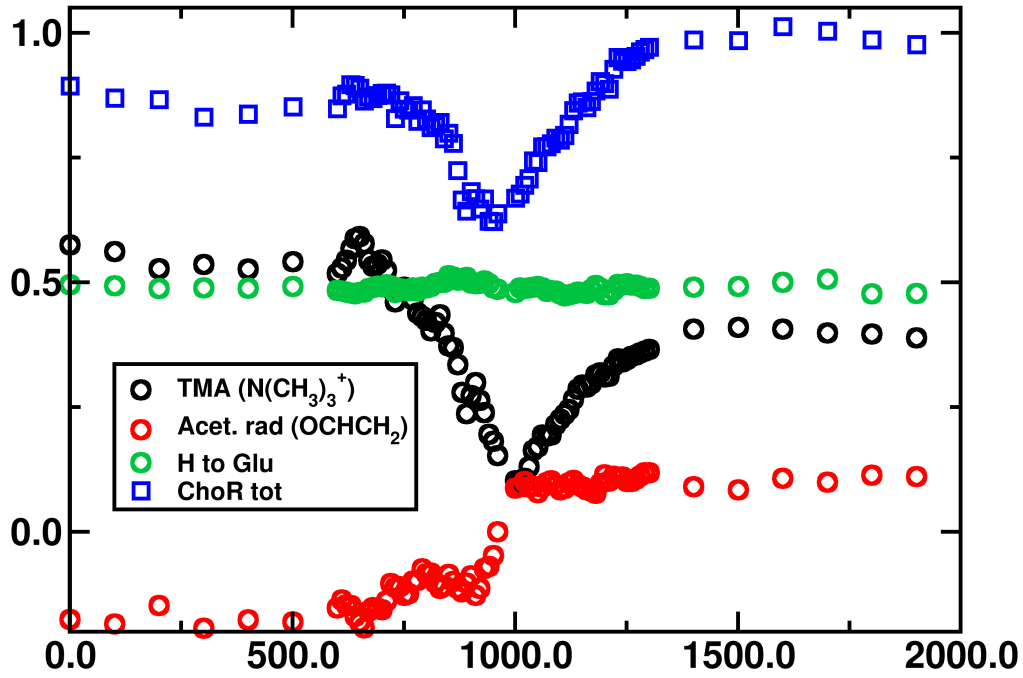

Figure S8. Charges of choline fragments during forced protonation.

Table S9. Summary of close contacts and C-H···O interactions in the CutC crystal structure.

			Total interaction energies (kcal/mol)			
Res 1 (atom)	Res 2 (atom)	Distance (Å)	B3LYP	SAPT0	MM	QTAIM E_{HB} (kcal/mol)
GLU279(OE1)	ARG48(NH2)	2.6	-38.4	-97.6	-88.3	-18.8
GLU776(OE2)	ARG78(NH2)	2.4	-42.0	-109.2	-80.0	-33.0
TYR340(OH)	PRO105(O)	2.6	-11.5	-9.0	-8.2	-14.2
LYS113(NZ)	GLU110(OE2)	2.6	-56.0	-130.9	-113.2	-21.3
MET536(O)	TYR206(OH)	2.6	-7.1	-6.4	-8.7	-16.3
TYR549(OH)	ASP428(OD2)	2.6	-20.4	-26.0	-17.9	-17.5
THR450(OG1)	GLU439(OE2)	2.6	-18.9	-23.7	-19.2	-18.5
ARG502(NH1)	GLU499(OE2)	2.5	-45.5	-111.0	-87.4	-33.7
THR636(OG1)	GLY552(O)	2.5	-3.8	-2.5	-4.6	-14.4
TYR615(OH)	ASP576(OD2)	2.4	-16.5	-24.1	-16.2	-27.0
ASP602(OD2)	TYR580(OH)	2.6	-17.6	-23.0	-15.5	-16.4
THR629(OG1)	PHE626(O)	2.5	-5.1	-2.5	-4.4	-10.9
GLN741(NE2)	GLU739(OE2)	2.5	-18.7	-31.2	-22.0	-21.9
TYR760(OH)	ASP752(OD2)	2.5	-23.7	-31.3	-21.5	-19.9
SER787(OG)	GLU784(O)	2.5	-10.0	-12.7	-15.3	-17.6
CHT795(C7)	ASH164(OD1)	3.2	-5.9	-6.7	-3.2	-4.0
CHT795(C6)	TYR156(OH)	3.4	-5.7	-7.1	-4.6	-3.6
CHT795(C7)	THR450(OG1)	3.7	-3.3	-2.9	-1.7	-0.7

Text S1. Additional details about close contact analysis of CutC.

The interaction energies of the 15 close contact pairs in the CutC crystal structure range from -2.5 kcal/mol to -130.9 kcal/mol for SAPT0, from -3.8 kcal/mol to -56.0 kcal/mol for B3LYP, and from -4.4 kcal/mol to -113.2 kcal/mol for AMBER. The B3LYP energy range is much narrower than the SAPT0 energy range because it is calculated in dielectric, which attenuates interactions. The three methods give well-correlated energies, with R^2 values for linear regression ranging from 0.94 to 0.98; the two QM methods gave the highest R^2 value. For all the close contacts, we locate bond critical points between the hypothesized hydrogen bond donor and

acceptor using QTAIM theory. The hydrogen bond energies, using the estimate of one half of the potential density at the bond critical point, range from -10.9 kcal/mol to -33.7 kcal/mol. The BCP energies are somewhat correlated with the overall interaction energy, with R^2 values for linear regression ranging from 0.40 to 0.52. We also examine the three CHO hydrogen bonds that choline makes with nearby residues. These three interactions are longer than the close contacts, at 3.21 Å to 3.71 Å, and give correspondingly weaker interactions, with SAPT0 interaction energies ranging from -2.9 kcal/mol to 7.1 kcal/mol, B3LYP interaction energies ranging from -3.3 kcal/mol to -5.9 kcal/mol, and MM interaction energies ranging from -1.7 kcal/mol to -4.6 kcal/mol. For DNMT1, One challenge for simulating DNMT1 is the relatively low resolution of crystal structures and difficulty associated with solving crystal structures with multiple cofactors bound. In the initial structure of DMNT, 100 close contact residue pairs are observed, but only around 25% have favorable interaction energies when evaluated with wavefunction theory (i.e., SAPT0) or DFT (i.e., B3LYP) (see session file provided in the ESI). It can be essential to carry out MD equilibration to improve the structure, but is known to not always lead to good treatment of non-covalent interactions. After equilibration, only five close contact residue pairs are observed, all with favorable interaction energies that correspond to likely hydrogen bonds. However, none of these close contacts were present in the initial crystal structure.

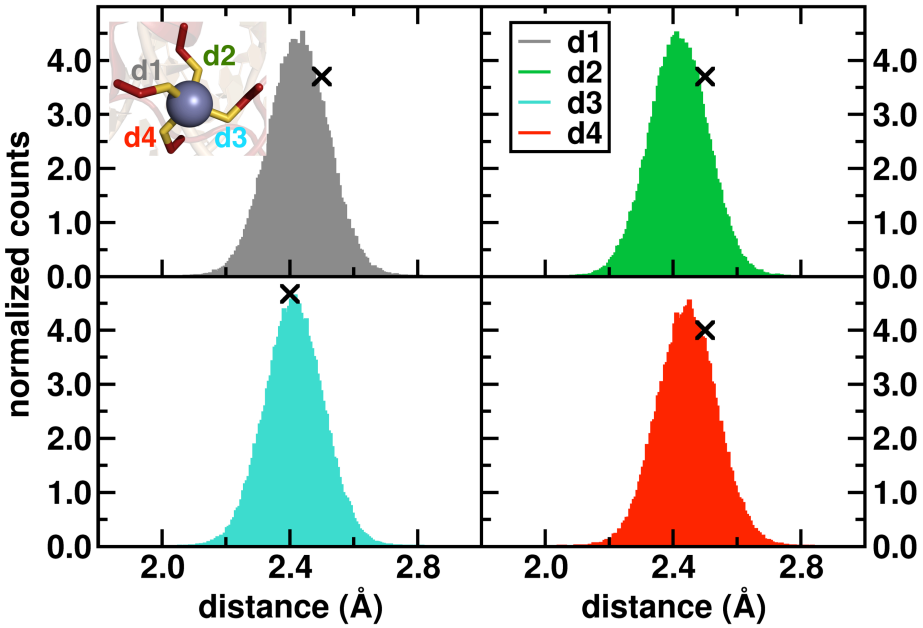

Figure S9. Bond distances d1, d2, d3 and d4 sampled between Zn2 and Cys13, Cys16, Cys19 and Cys51 (shown in colors gray, green, turquoise and red) respectively during 250 ns of production dynamics. The black crosses represent bond lengths obtained from QM-only optimizations of smaller cluster models containing 299 atoms.

Table S10. Radially-sized QM regions selected by including entire residues if any atom was within a fixed distance to the Zn^{2+} center of the Zn2 site for 7 QM regions and distance cutoffs up to 10 Å. The QM region 5 was selected for QM-only cluster optimizations referred to in the main text. Each QM region is indicated by "Y" for residues included in it along with a total number of atoms, number of atoms including link hydrogen atoms, and the resulting net charge.

Residue	#At	Chg.	**1** (3 Å)	**2** (5 Å)	**3** (6 Å)	**4** (7 Å)	**5** (8 Å)	**6** (9 Å)	**7** (10 Å)
Zn2	1	2	Y	Y	Y	Y	Y	Y	Y
Arg11	24	1					Y	Y	Y
Arg12	24	1		Y	Y	Y	Y	Y	Y
Cys13	10	-1	Y	Y	Y	Y	Y	Y	Y
Gly14	7	0		Y	Y	Y	Y	Y	Y
Val15	16	0		Y	Y	Y	Y	Y	Y
Cys16	10	-1	Y	Y	Y	Y	Y	Y	Y
Glu17	15	-1			Y	Y	Y	Y	Y
Val18	16	0		Y	Y	Y	Y	Y	Y
Cys19	10	-1	Y	Y	Y	Y	Y	Y	Y
Gln20	17	0			Y	Y	Y	Y	Y
Gln21	17	0					Y	Y	Y
Glu48	15	-1							Y
Arg49	24	1				Y	Y	Y	Y
Arg50	24	1				Y	Y	Y	Y
Cys51	10	-1	Y	Y	Y	Y	Y	Y	Y
Pro52	14	0		Y	Y	Y	Y	Y	Y
Asn53	14	0		Y	Y	Y	Y	Y	Y
Met54	17	0			Y	Y	Y	Y	Y
Ala55	10	0					Y	Y	Y
Lys775	22	1							Y
Phe852	20	0							Y
Cys859	11	0							Y
Asn889	14	0							Y
Glu891	15	-1					Y	Y	Y
Met893	17	0						Y	Y
Gly894	7	0							Y
Totals									
# At.			41	132	181	229	295	312	401
# At. w/ link			49	138	185	233	299	320	417
Charge			-2	-1	-2	0	0	0	0

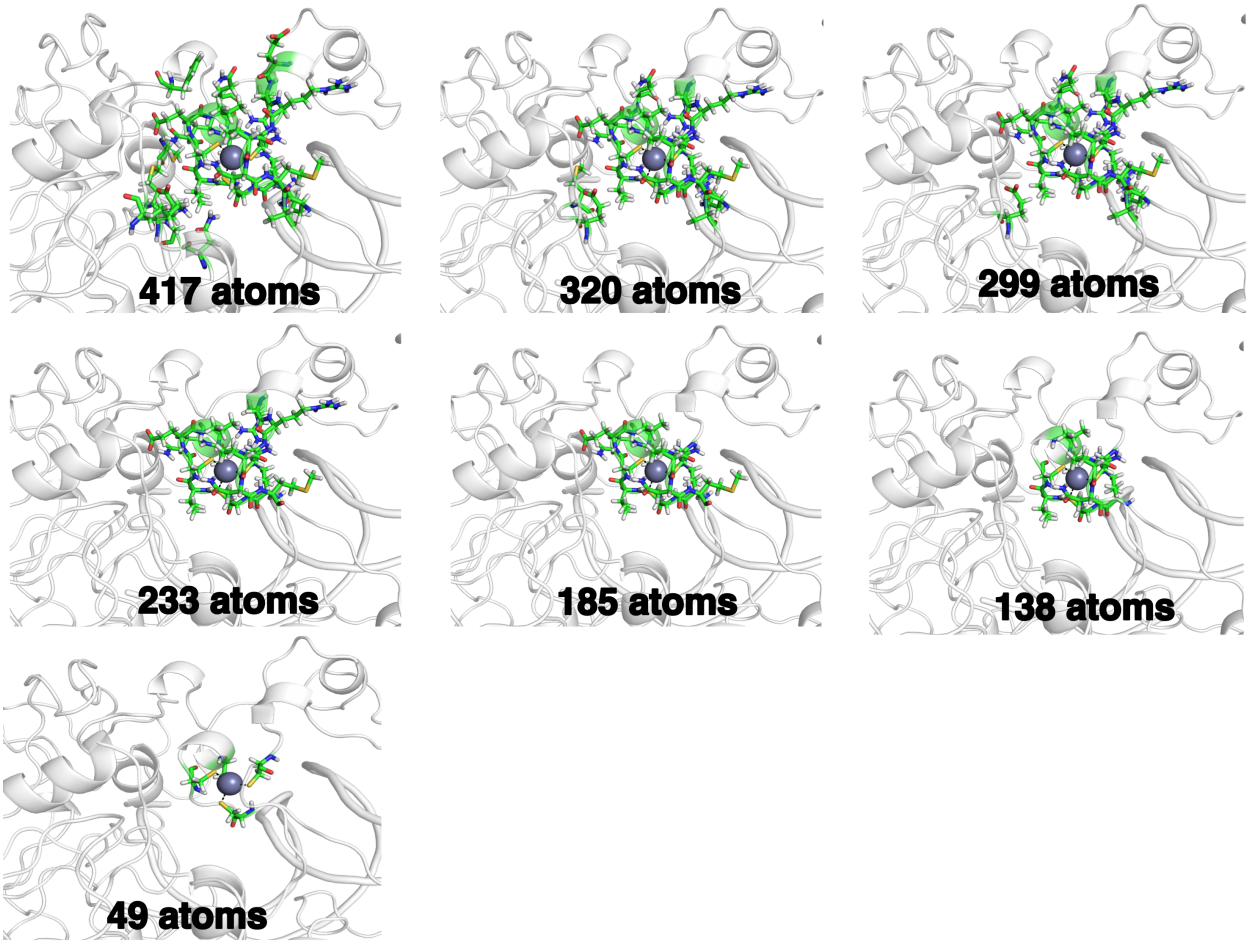

Figure S10. Stick representation models of QM residues in QM regions for Zn2 with number of atoms including link atoms shown in insets. The residues in QM region are shown as colored sticks, and the surrounding protein treated with MM is shown as grey cartoon. The bonds between zinc ions and coordinating residues are shown as dashed black lines.

Table S11. Charge redistribution upon removal of Zn from Zn2 site with largest QM region containing 417 atoms for snapshot at 34 ns from production dynamics of DNMT. $q_{Zn\text{-}DNMT}$ represents charge on residue in presence of Zn2, q_{DNMT} represents charge on residue after zinc removal and the difference is given as Δq.

Residue	$q_{Zn\text{-}DNMT}$	q_{DNMT}	Δq
ZN2	0.49	-	-
ARG11	0.60	0.57	0.03
ARG12	0.85	0.65	0.20
CYS13	-0.57	-0.81	0.24
GLY14	0.01	-0.03	0.05
VAL15	-0.05	-0.13	0.09
CYS16	-0.56	-0.68	0.11
GLU17	-0.99	-1.09	0.10
VAL18	0.03	-0.05	0.08
CYS19	-0.65	-0.70	0.05
GLN20	-0.06	-0.12	0.06
GLN21	-0.19	-0.18	-0.01
GLU48	-1.43	-1.45	0.02
ARG49	1.00	1.01	-0.01
ARG50	0.99	0.91	0.08
CYS51	-0.52	-0.70	0.18
PRO52	0.02	-0.08	0.10
ASN53	0.01	-0.02	0.04
MET54	-0.07	-0.09	0.02
ALA55	-0.06	-0.06	0.00
LYS775	0.46	0.46	0.00
PHE852	-0.46	-0.46	0.00
CYS859	-0.53	-0.53	-0.01
ASN889	-0.54	-0.53	-0.02
GLU891	-1.54	-1.53	-0.01
MET893	-0.46	-0.46	0.00
GLY894	-0.12	-0.12	0.00